PUBLICATIONS OF THE ASTRONOMICAL SOCIETY OF THE PACIFIC, **121**:260–265, 2009 March

A Micro Electrical Mechanical Systems (MEMS)-based Cryogenic Deformable Mirror

K. ENYA,[1] H. KATAZA,[1] AND P. BIERDEN[2]

enya@ir.isas.jaxa.jp

Received 2008 June 14; accepted 2009 February 11; published 2009 March 26

ABSTRACT. We present our first results on the development and evaluation of a cryogenic deformable mirror (DM) based on Micro Electro Mechanical Systems (MEMS) technology. A MEMS silicon-based DM chip with 32 channels, in which each channel is $300\ \mu\text{m} \times 300\ \mu\text{m}$ in size, was mounted on a silicon substrate in order to minimize distortion and prevent it from being permanently damaged by thermal stresses introduced by cooling. The silicon substrate was oxidized to obtain electric insulation and had a metal fan-out pattern on the surface. For cryogenic tests, we constructed a measurement system consisting of a Fizeau interferometer, a cryostat cooled by liquid N_2, zooming optics, electric drivers. The surface of the mirror at 95 K deformed in response to the application of a voltage, and no significant difference was found between the deformation at 95 K and that at room temperature. The power dissipation by the cryogenic DM was also measured, and we suggest that this is small enough for it to be used in a space cryogenic telescope. The properties of the DM remained unchanged after five cycles of vacuum pumping, cooling, warming, and venting. We conclude that fabricating cryogenic DMs employing MEMS technology is a promising approach. Therefore, we intend to develop a more sophisticated device for actual use, and to look for potential applications including the Space Infrared Telescope for Cosmology & Astrophysics (SPICA), and other missions.

1. INTRODUCTION

The development of large space-borne cooled telescopes is essential for progress to be made in infrared astronomy and astrophysics. Space telescopes are free from wavefront turbulence, constraints on the wavelengths that can be observed, and thermal background caused by the atmosphere of the earth. Improving the sensitivity of a space-borne infrared telescope requires cooling to reduce the thermal infrared background emitted from the telescope itself. Table 1 shows the infrared space telescopes currently in orbit and those planned for future missions.

In developing space telescopes, one of the most important issues that needs to be addressed is how one reduces and controls the deformation of telescopes with light-weight mirrors to obtain a required wavefront, which normally corresponds to the diffraction-limited resolution determined by telescope aperture size. Once in orbit, the space telescope is released from the gravitational effects of the earth, which inevitably leads to deformation. If the telescope is cooled, thermal deformation due to mismatched coefficients of thermal expansion (CTE) in the telescope materials can be a serious issue. These difficulties increase the cost and time needed to design, manufacture, evaluate, and guarantee the final performance of space telescopes.

By adding a small active optics device to the space-borne infrared telescope, the specification for the wavefront by the telescope itself can be relaxed, and the reliability of the whole telescope system can be increased. One such device is a deformable mirror (DM) that can be operated at cryogenic temperatures (Dyson et al. 2001; Mulvihill et al. 2003). One of the more usual types of DM is based on the piezoelectric effect; however, this effect tends to be smaller at cryogenic temperatures (the piezoelectric coefficient at 5 K is $\sim 1/10$ of that at ambient temperature: see also Mulvihill et al. 2003). Recently, DMs fabricated using Micro Electro Mechanical Systems (MEMS) techniques have been developed (e.g., Biffano et al. 1997; Stewart et al. 2007). Operation of the MEMS DM is based on Coulomb forces, so does not depend on the piezoelectric effect. The potential to realize large format and compact DMs is also an advantage of MEMS technology. For example, MEMS DMs in the ~ 1 cm size range with 32×32 channels are commercially available.

In general, the required properties of DMs for the cryogenic space-borne infrared telescope tend to be common (e.g, reliable operation in cryogenic systems, channel stroke that exceeds expected wavefront error, channel control resolution and accuracy that exceeds required final wavefront, and compactness), while the specific values for these requirements completely depend on the specific nature of each mission; Table 1 shows some

[1] Department of Infrared Astrophysics, Institute of Space and Astronautical Science, Japan Aerospace Exploration Agency, 3-1-1 Yoshinodai, Sagamihara, Kanagawa 229-8510, Japan

[2] Boston Micromachines Corporation, Cambridge, MA 02138

TABLE 1

SPACE TELESCOPES FOR INFRARED ASTRONOMY, CURRENTLY IN ORBIT OR PLANNED FOR FUTURE MISSIONS

Telescope[a]	Launch[b]	D[c] (m)	λ[d] (μm)	T[e] (K)
Spitzer Space Telescope	2003	0.85	3–180	~5.5
AKARI	2006	0.7	1.7–180	~6
Herschel Space Observatory	(2009)	3.5	60–670	~80
JWST	(2013)	6.5	0.6–27	50
SPICA	(2017)	3.5	5–200	~5

[a] JWST, James Webb Space Observatory; SPICA, Space Infrared Telescope for Cosmology; AKARI satellite.

[b] Launch year for the Spitzer Space Telescope and AKARI, planned launch year for the others.

[c] Entrance pupil diameter.

[d] Core wavelength of observation.

[e] Temperature of telescope before running out of cryogen. REFERENCES.—Spitzer Space Telescope, Werner et al. 2004; Gehrz et al. 2004; AKARI, Murakami et al. 2007; Kaneda et al. 2007; Herschel Space Observatory, Sein et al. 2003; JWST, Sabelhaus &Decker 2004; SPICA, Nakagawa & Murakami 2007; Onaka & Nakagawa 2005.

examples. Among the missions listed, the Space Infrared Telescope for Cosmology & Astrophysics (SPICA) mission is one of the most interesting platforms for us (Nakagawa & Murakami 2007; Onaka & Nakagawa 2005). The wavefront specification of the SPICA telescope itself is 350 nm rms, which corresponds to diffraction-limited imaging at 5 μm wavelength. In the case of the midinfrared instruments, including the coronagraph, it is potentially beneficial to correct the wavefront to 70 nm rms to extend the diffraction-limited observation toward the 1 μm wavelength level, where an InSb detector has significant sensitivity (coronagraph optics requires more stringent specifications, which are discussed in § 4). A DM for SPICA has to work at 5 K, with a required cancel stroke of 1.5 μm, and the maximum size of the DM should be ~1 cm. Operation frequency is almost at the DC level, because the telescope is free from atmospheric turbulence, while power dissipation is strictly limited to be smaller than 1 mW. We found that in principle, MEMS DMs had the potential to satisfy such requirements for SPICA and other missions.

However, the stress introduced into MEMS DMs by cooling, due to mismatched coefficients of thermal expansion (CTE), can cause distortion and even destroy the mirror. Hence, we intended to develop and evaluate a prototype cryogenic DM system based on MEMS and mounted on a special substrate designed to reduce thermal stress.

2. MANUFACTURING THE PROTOTYPE DM

The structure of the prototype DM unit is shown in Figure 1. Figure 1a is a schematic view of the MEMS DM chip used for the prototype DM unit. The chip, which was made by the Boston Micromachines Corporation (BMC), had a continuous surface with a channel pitch of 300 μm and the maximum channel

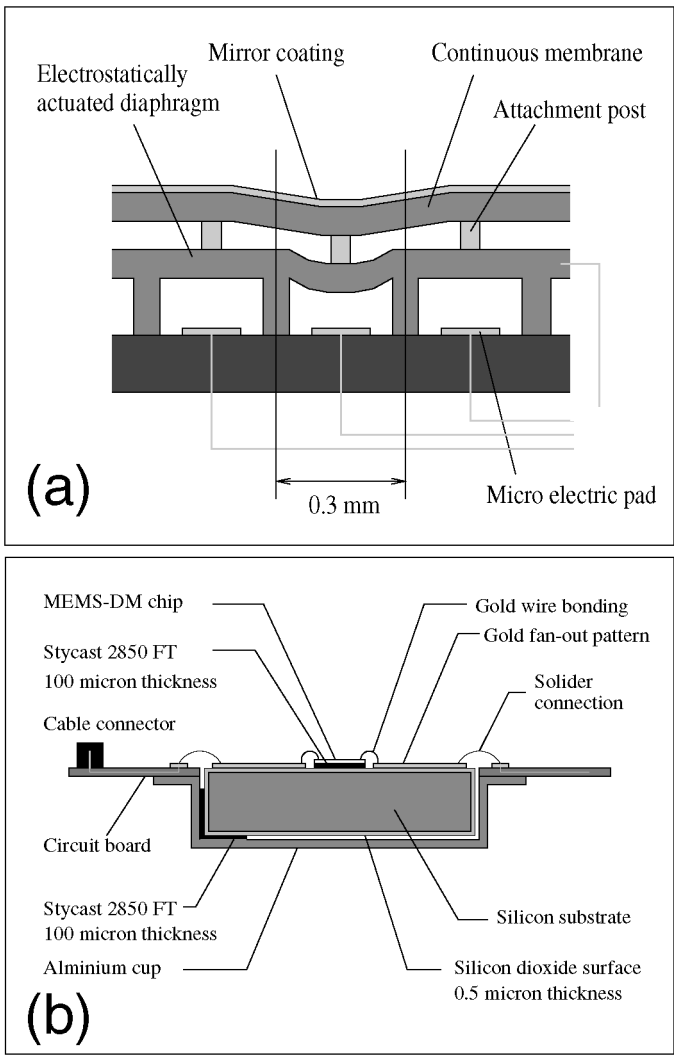

FIG. 1.—(*a*) Schematic view of the structure of the MEMS chip. (*b*) Schematic view of the prototype DM unit. (*c*) The DM unit installed in a cryostat. The radiation shield and temperature sensor are not shown in this photograph.

stroke of 1.5 μm (Bifano et al. 1997). The mirror surface of the chip was coated with gold. Each channel of the DM chip is actuated by applied voltage between the diaphragm, which is electrically common, and micro electric pads are prepared for each channel. The DM chip we used for our prototype DM unit is essentially the same as chips for commercially available DMs. However, the typical commercially-available DMs have a complicated structure that includes a ceramic substrate with many electric pins, a plastic socket, cover glass to protect the DM chip set on the substrate, and glue to support the structure.

The main objective in the design of the prototype DM in this work was to reduce the thermal stress caused by the use of various materials and the structure of typical DM units, when the unit is cooled to cryogenic temperatures. Because the MEMS DM chip is mainly made of silicon, our fan-out board was also made from silicon in order to minimize thermal stress. The size of the silicon substrate was 50 mm $\times$ 50 mm $\times$ 10 mm. This substrate was oxidized to form an insulating silicon dioxide layer on the surface, using a thermal oxidation furnace at the Center for International Research on MicroMechatronics, Institute of Industrial Science, University of Tokyo. Oxidation was carried out in an oxygen ambient of 1 atm, at a temperature of 1000°C for 4 hr. The thickness of the silicon dioxide was expected to be $\sim$0.5 μm. After oxidation, a fan-out pattern in gold was fabricated on the surface by photolithography. The substrate with the fan-out pattern was glued inside an aluminum cup using Stycast 2850 FT adhesive. The Stycast 2850 FT was used only within 10 mm of one corner of the substrate to prevent thermal stresses from affecting the central part of it. A circuit board surrounding the substrate was fixed to the aluminum cup by screws. The outer terminals of the fan-out pattern were connected to terminals on the circuit board by copper wire and solder. The substrate unit was then sent to BMC to complete the manufacturing.

At BMC, the MEMS chip was glued with a $\sim$100 μm layer of Stycast 2850 FT onto the center of the fan-out board. For this prototype, we used a 12 $\times$ 12 channel MEMS DM chip; however, to make the manufacturing process simpler, only the central 32 channels were completed. No window was attached to cover the chip during the cryogenic tests in vacuum, whereas there would usually be a window with nitrogen gas filling the space between the chip and the window. The terminals on the outer part of the MEMS chip were connected to terminals on the fan-out pattern by gold wire bonding. The prototype DM unit was then sent back to the Institute of Space and Astronautical Science, Japan Aerospace Exploration Agency (ISAS/JAXA) for cryogenic tests.

3. CRYOGENIC TESTS AND RESULTS

3.1. Configuration

One of the key issues to address was how we should measure the surface figure of a very small DM set in cryostat. Figure 2 shows the setup of the experimental system. This consists of the prototype DM unit, a cryostat cooled by liquid nitrogen, a Fizeau interferometer (Zygo GPI-XP), zooming optics, and a commercially available DM driver produced by BMC. This was all set on an air-suspension table, and the entire system was set in a clean booth with a HEPA filter.

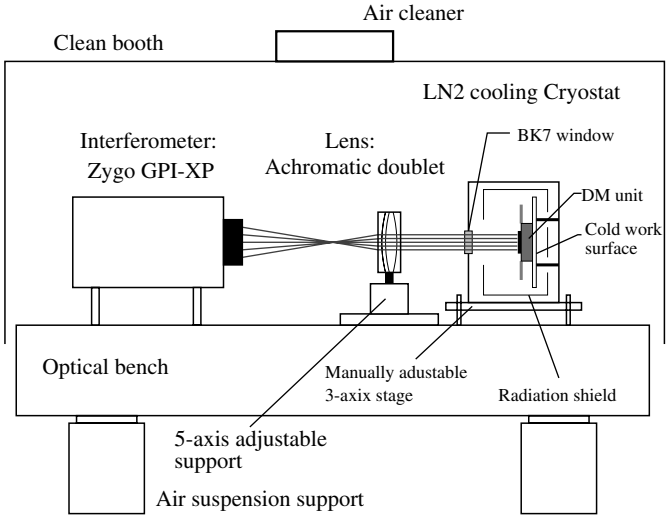

FIG. 2.—Schematic view of measurement setup.

The DM unit was set on a work surface covered by radiation shields in the cryostat throughout all tests. The work surface and the radiation shields were cooled through thermal conductance by a heat strap connected to a tank of liquid nitrogen. A molecule absorber made of charcoal was attached to the liquid nitrogen tank. The cooled absorber kept the cryostat under vacuum, even after the vacuum pumping was stopped in order to avoid vibration caused by the pump, to achieve the stability needed for interferometric measurement. The heat strap was removable so that not only the cryogenic test, but also the room temperature test of the DM could be performed with the advantage of the cooled absorber. The cryostat had a flat BK7 glass window through which the beam from the interferometer was introduced. A broadband Multiple Layer Anti-Reflection (BMLAR) coating optimized for the 400–700 μm wavelength region was applied to both sides of the window. The temperature of the silicon dioxide surface on the fan-out board was monitored with a platinum resistance thermometer. The cryostat was supported such that the height, and the tip and tilt angles could be manually adjusted.

We used a focusing beam provided by the interferometer with a f/7.2 Fizeau lens. An achromatic doublet (i.e., cemented by optical contact) lens of 50 mm diameter and f = 150 mm was used in the zooming optics to collimate the beam. A BMLAR coating was also applied to both sides of the lens, which was mounted on a motor-driven mechanical stage that could be adjusted with 5 degrees of freedom: x, y, and z axes, and the tip and tilt angles.

A commercially available driver system from BMC was used to deform the DM in the cryostat.

3.2. Surface Deformation Measurement

First, we estimated the systematic error in the surface figure measurement due to aberration, multireflection, and so on, by the zooming optics and distortion of the cryostat window by atmospheric pressure when the cryostat was under vacuum. Using an optically-flat reference mirror, we confirmed that the systematic error in measuring the global surface figure was smaller than 5 nm PV for the area corresponding to the central 32 active channels of the DM chip, regardless of the vacuum pumping and cooling of the cryostat. This systematic error is significantly smaller than the maximum channel stroke.

Next, we carried out a deformation test of the DM at room temperature in the vacuum cryostat. The DM unit was installed with the aluminum cup in contact with the work surface of the cryostat, but with the heat strap removed. The cryostat was pumped continuously for 24 hr, and then liquid nitrogen was poured into the tank to cool a charcoal molecular absorber attached to the tank. The vacuum valve on the cryostat was closed and the pump was disconnected from the measurement system. As a result, vibration from the pump was eliminated and interferometric measurements became possible. Figure 3a shows the surface figure data obtained from the interferometer, of the DM chip at room temperature before the application of a voltage to any of the channels. Then a voltage was applied to the thirteenth channel to evaluate the relationship between voltage and the deformation depth, as shown in Figure 4. This was evaluated both with increasing and decreasing voltage to check for hysteresis. Thanks to the absorber, it was possible to maintain a vacuum of $\sim 10^{-6}$ torr in the cryostat during the measurement, while the temperature of the silicon substrate was $20 \sim 18$°C.

After the test at room temperature, we performed a deformation test at cryogenic temperatures. The cryostat was opened and the heat strap was attached to change the setup to cool the work surface and radiation shield by liquid nitrogen through the strap. After 24 hr cooling, the temperature of the fan-out board had reached 95 K. After the vacuum valve was closed and the pump was removed from the setup, interferometric measurements were carried out. Figure 3b shows the surface figure data of the DM chip at 95 K without voltages applied. Both the cryogenic and the room temperature figure of the deformable area of the DM chip evaluated as residual from a flat plane was ~7 nm rms, and the difference between the cryogenic and the room temperature figure was smaller than the channel stroke of the DM. This result suggests that the surface flatness of the DM was sufficiently maintained for use though the cooling process. We then performed a deformation test of the cooled DM, with the same procedure used for the room temperature test. Figure 3c and 3d show examples of the interferometric data from our first deformation test on the cryogenic DM.

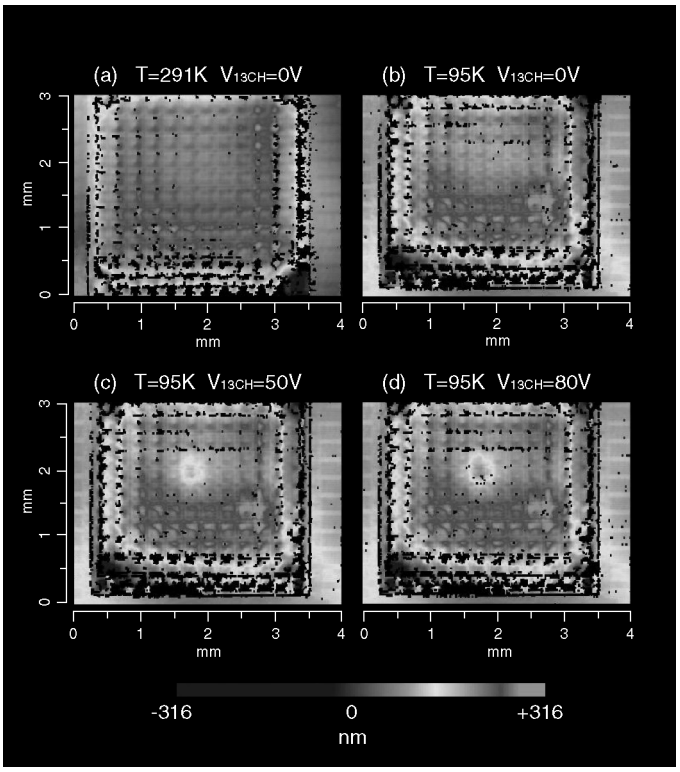

FIG. 3.—3D surface data obtained from the interferometer. All data were obtained by measurements made through the window of the vacuum cryostat. (*a*) Surface without applied voltage at room temperature. (*b*) Surface without applied voltage at 95 K. (*c*) Surface with 50 V on the thirteenth CH at 95 K. (*d*) Surface with 80 V on the thirteenth CH at 95 K. The difference between (*a*) and (*b*) is much smaller than the channel stroke of deformation caused by the voltage applied.

The obtained relationship between the applied voltage and the deformation depth is shown in Figure 4. The nonlinear relationship between the voltage and the deformation depth is consistent with that of commercially available devices, which is expected as Coulomb force is enhanced when distance between the diaphragm and the micro electric pad becomes closer. We evaluated the measurement accuracy of the deformation depth as ~10 nm rms from repeatability of measurements for nondeformable parts of the device with similar scale to the deformation. This suggested that the measurement accuracy for steep structures with small spatial scale is not as high as that for the smooth surface of the optically flat reference mirror. Indeed, when voltage higher than ~100 V was applied, the interferometric measurement failed because the continuous phase scan was interrupted by the steep surface. For this reason, the applied voltage was constrained to below 80 V. The limiting factor of the repeatability of the deformation depth measurement was not fixed, while we considered slight mechanical vibration, air turbulence, and/or aliasing of the interferometric measurement as possible causes of the limiting factor. Within the measurement

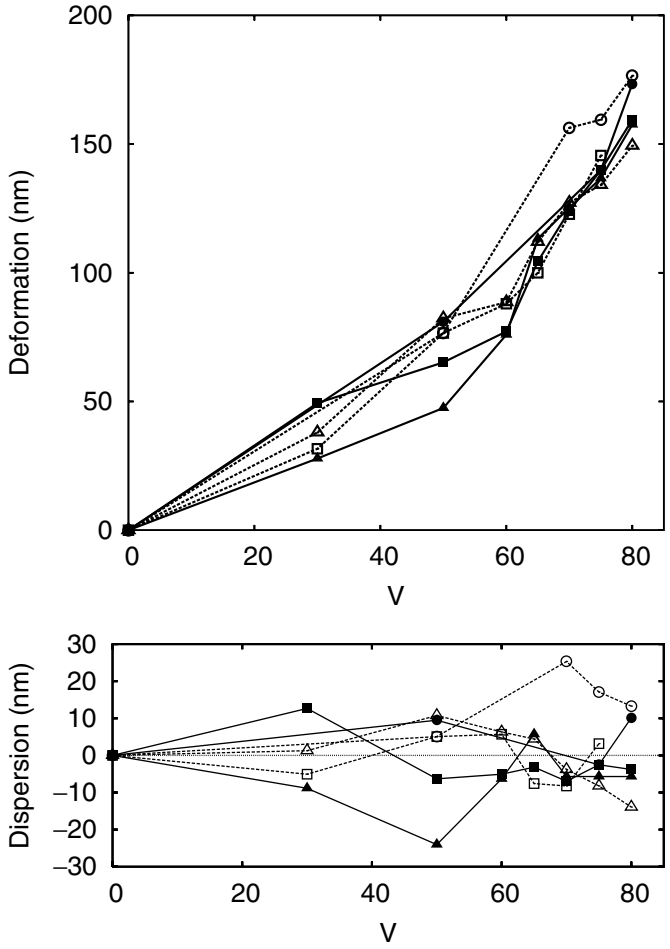

FIG. 4.—Relationship between the applied voltage and the deformation depth. *Circle:* Room temperature, before cooling. *Rectangle:* 95 K. *Triangle:* Room temperature, after the load cycle test. *Solid symbols:* data obtained with increasing voltages; *empty symbols:* data obtained with decreasing voltages. Depth = 0 nm is for the case of V = 0.

accuracy, any significant change due to cooling was found in the relationship between the applied voltage and the deformation depth. In addition, no significant hysteresis was found in the data in Figure 4.

3.3. Power Dissipation Test

The amount of power dissipation by the DM is critical for its use with a cryogenic space telescope, because the total cooling power for all the cooled instruments is strictly limited. We installed a digital ammeter to measure the electric current in the common ground line of a cable to drive the DM, and applied the maximum voltage, DC 200 V, to all channels. No significant current was detected in this test. A conservative estimation of the upper limit of the total current is $I_u \sim 3 \times 10^{-10}$ A/Ch.

3.4. Load Cycle Test

Robustness against vacuum pumping and the cooling cycle is another important property. We applied five cycles to the cryostat with the DM unit, in which each cycle consisted of vacuum pumping, cooling with liquid nitrogen, warming up, and venting the cryostat back to 1 atm. Afterward, the cryogenic deformation test was carried out using the same procedure described in Section 3.2, which confirmed that all the channels could still be normally deformed as shown in the first test. The relationship between the applied voltage and the deformation depth was measured again at room temperature, as shown in Figure 4, and it was confirmed that no significant change in the relationship was introduced as a result of the load cycle test.

4. DISCUSSION

As described in § 3, it was shown in the first results from our development and evaluation of a cryogenic MEMS DM that the DM worked at cryogenic temperature with neither destruction nor significant change of its properties. The obtained property of the channel actuation satisfied the specification needed for the midinfrared instrument of SPICA, though directly confirmed temperature coverage and channel stroke were limited. These results suggest that using MEMS technology is potentially a useful manufacturing method to realize a cryogenic DM.

One of the important issues to address following this work is enlarging the format of the MEMS chip from 32 channels to, for example, $32 \times 32 = 1024$ channels for practical use in an astronomical instrument for SPICA and other telescopes. Development of a more sophisticated gluing process and a new design of the substrate structure may be needed to complete the development of a flat DM with a larger format at cryogenic temperatures. Finally, the measurement system needs to be expanded to carry out tests on larger DM chips cooled by liquid helium at 4.2 K.

It was shown that measurement of the power dissipation in this work was sufficiently sensitive to check the DC operation. We estimate the upper limit to the power dissipation by a DM with 1024 channels to be $200\ \mathrm{V} \times I_u \mathrm{A/Ch} \times 1024\ \mathrm{Ch} \sim 6 \times 10^{-5}$ W. This value satisfies the requirement for the SPICA mission, which is less than 1 mW. On the other hand, if we intend to apply the DM to real-time dynamic wavefront corrections such as adaptive optics used to correct air turbulence for a ground-based telescope, a more extensive evaluation is needed.

The coronagraph optics of SPICA, which provide optional function in the midinfrared instrument, require more stringent specifications to produce the high-contrast images needed for direct detection of extrasolar planets (Enya et al. 2006, 2007; Abe et al. 2007). The typical required accuracy of the channel actuation is several nm rms or less, whereas it depends on the observation wavelength. Therefore, we need more precise methods to evaluate the surface deformation than those described

in this work, if we intend to confirm the properties of the cryogenic DM for the SPICA coronagraph. It should be noted that the contrast of 6.5×10^{-7} was achieved in a laboratory experiment at room temperature using visible laser with 632.8 nm wavelength using a commercially available MEMS DM from the BMC (Tanaka et al. 2007). This contrast is better than the requirement of the SPICA coronagraph, 10^{-6}. Because the needed actuation accuracy to realize a fixed contrast (e.g., 10^{-6}) is relatively higher at shorter wavelengths, the achieved surface accuracy of the DM in this experiment is also higher than the coronagraphic requirement for SPICA. Hence, if a MEMS DM chip works at cryogenic temperature as precisely as it did in the experiment at room temperature, it will be possible with the DM to achieve the required contrast for the SPICA coronagraph. In such case, finally the end-to-end demonstration of high contrast using a DM and coronagraph at cryogenic temperature will be able to guarantee the accuracy of the channel actuation, in which the coronagraph itself can be regarded as a high-sensitivity sensor of residual wavefront error.

Following this work, we are seeking an application for the cryogenic DM. If a DM with 1024 channels works at cryogenic temperatures down to 5 K, then this temperature coverage is enough for most infrared space telescopes. A MEMS chip with 6 μm maximum channel stroke is also available from BMC. Use of such large stroke chips has the potential to realize a cryogenic DM for space telescopes for observation at longer wavelength than SPICA, with the needed larger channel stroke and final residual wavefront. An application of the cryogenic DM as an internal device of a cooled camera and/or spectrometer for ground-based telescopes is also potentially useful.

5. CONCLUSION

We have presented the first demonstration of our cryogenic DM made using MEMS technology. This provides a promising method for fabricating cryogenic DMs. Following on from this work, a more sophisticated device for actual use needs to be developed, and a search to identify possible applications needs to be conducted.

We are grateful to M. Mita, T. Yamamuro, A. Suenaga, and M. Venet for their kind support. This work is supported by JAXA. The opportunity to use the interferometer was provided by the open use program of the Advanced Technology Center (ATC) of the National Astronomical Observatory of Japan. We would like to thank all persons in the ATC program, especially K. Mitsui and M. Yokota. We are grateful for fruitful referee comments and editorial work.

REFERENCES

Abe, L., Enya, K., Tanaka, S., Nakagawa, T., Kataza, H., Tamura, M., & Guyon, O. 2007, Comptes Rendus Physique, 8, 374

Bifano, T. G., Mali, R., Perreault, J., Dorton, K., Vandelli, N., Horentein, M., & Castan˜on, D. 1997, Opt. Eng., 36, 1354

Dyson, H., Sharples, R., Dipper, N., & Vdovin, G. 2001, Optics Express, 8, 17

Enya, K., Abe, L., Tanaka, S., Haze, K., Venet, M., Nakagawa, T., Kataza, H., Tamura, M., et al. 2007, Proc. SPIE, 6693, 0I1

Enya, K., Nakagawa, T., Kataza, H., Kaneda, H., Yui, Y. Y., Tamura, M., Abe, L., Obuchi, Y., et al. 2006, in IAU Colloq. 200, Direct Imaging of Exoplanets: Science & Techniques, ed. C. Aime, & F. Vakili (Cambridge: Cambridge Univ. Press), 467

Gehrz, R. D., Romana, E. A., Hoffmann, W. F., Schwenker, J. P., & Mentzell, J. E., et al. 2004, Proc. SPIE, 5487, 166

Kaneda, H., Kim, W., Onaka, T., Wada, T., Ita, Y., Sakon, I., & Takagi, T. 2007, PASJ, 59, 423

Mulvihill, M. L., Roche, M. E., Cavaco, J. L., Shawgo, R. J., Chaudhry, Z. A., & Ealey, M. A. 2003, Proc. SPIE, 5172, 60

Murakami, H., Baba, H., Barthel, P., Clements, D. L., & Cohen, M., et al. 2007, PASJ, 59, 369

Nakagawa, T., & Murakami, H. 2007, Adv. Space Res., 34, 645

Onaka, T., & Nakagawa, T. 2005, Adv. Space Res., 36, 1123

Sabelhaus, P. A., & Decker, J. 2004, Proc. SPIE, 5487, 550

Sein, E., Toulemont, Y., Safa, F., Duran, M., Deny, P., de Chambure, D., Passvogel, T., & Pilbratt, G. L. 2003, Proc. SPIE, 4850, 606

Stewart, J. B., Bifano, T. G., Cornelisse, S., Bierden, P., Levine, B. M., & Cook, T. 2007, Sensors and Actuators A: Physical, 138, 230

Tanaka, S., Guyon, O., Pluzhnik, E. A., Abe, L., Enya, K., & Nakagawa, T. 2007, in Spirit of Bernard Lyot: The Direct Detection of Planets and Circumstellar Disks in the 21st Century, ed. Kalas, Paul 41

Werner, M. W., Roellig, T. L., Low, F. J., Rieke, G. H., & Rieke, M., et al. 2004, ApJS, 154, 1